EXAFS investigation of UF_4

J. G. Tobin, C. H. Booth, W. Siekhaus, and D. K. Shuh

Citation: Journal of Vacuum Science & Technology A: Vacuum, Surfaces, and Films **33**, 033001 (2015);
View online: https://doi.org/10.1116/1.4915893
View Table of Contents: http://avs.scitation.org/toc/jva/33/3
Published by the American Vacuum Society

BRIEF REPORTS AND COMMENTS

This section is intended for the publication of (1) brief reports which do not require the formal structure of regular journal articles, and (2) comments on items previously published in the journal.

EXAFS investigation of UF_4

J. G. Tobin[a)]
Lawrence Livermore National Laboratory, Livermore, California 94550

C. H. Booth
Lawrence Berkeley National Laboratory, Berkeley, California 94720

W. Siekhaus
Lawrence Livermore National Laboratory, Livermore, California 94550

D. K. Shuh
Lawrence Berkeley National Laboratory, Berkeley, California 94720

(Received 9 January 2015; accepted 3 March 2015; published 19 March 2015)
[http://dx.doi.org/10.1116/1.4915893]

As part of our studies of 5f covalency in uranium compounds, a comparative structural study of UF_4 and UO_2, using extended x-ray absorption fine structure (EXAFS) and x-ray absorption near edge structure (XANES) techniques, was performed. This work confirms the quality of our samples and provides additional insight into geometrical issues related to ionicity and covalency. The local structure of UF_4 from EXAFS is consistent with the long range structure derived from diffraction data.

Actinide compounds, particularly actinide dioxides, have a propensity to exhibit covalency in their bonds.[1] Previously, a variety of soft x-ray techniques, including x-ray absorption spectroscopy,[2] bremsstrahlung isochromat spectroscopy,[2] resonant inverse photoelectron spectroscopy,[3] and x-ray emission spectroscopy (XES)[3,4] have been used to investigate uranium dioxide (UO_2). Now, as a further test of these analytical methods and the interplay of ionicity and covalency in actinide compounds, the studies are being expanded to include uranium tetrafluoride (UF_4). UO_2 and UF_4 are isoelectronic in terms of their formal charge states, i.e., U^{+4}, and they make for an interesting comparison in terms of covalency and ionicity, respectively. However, this comparison is complicated by significant structural differences: UO_2 is in a highly ordered, single site (fluorite) structure[5,6] and UF_4 is monoclinic with two U sites, as shown in Fig. 1.[7] The possibility of changes in the electronic structure are pursued in the XANES measurements (Fig. 2), while the structural difference is addressed with the EXAFS (Fig. 3) experiment.

U L_{III}-edge data were collected in fluorescence mode from the U L_α line (about 13.6 keV) on BL 11–2 (Ref. 8) at the Stanford Synchrotron Radiation Lightsource using a half-tuned double Si(220) ($\varphi = 0°$) LN_2-cooled monochromator on unfocused beam and a 100-element Ge solid-state detector.[9] The solid samples were placed in a LHe-flow cryostat, and all data were collected at T = 50 K. Data were processed using standard procedures and the RSXAP analysis package[10–12] with scattering functions generated by the FEFF8 code.[13] Data were corrected for dead time of the Ge detector. XANES data were energy calibrated by setting the first inflection point of the UO_2 spectrum to 17 166.0 eV. These data were normalized and corrected for self-absorption using the FLUO code.[14] A self-absorption correction was also applied to the EXAFS data[15] (factor of about 1.40 at 5 $Å^{-1}$). The EXAFS function $\chi(k) = (I_f(k) - I_0(k))/I_0(k)$ was determined from the measured fluorescence intensity $I_f(k)$ and the so-called "embedded atom" fluorescence $I_0(k)$ (analogous to the embedded atom absorption μ_α) as a function of the wave vector $k = [(2\,m_e/\hbar^2)(E - E_0)]^{1/2}$, where m_e is the rest mass of the electron, E is the incident photon energy, and the threshold energy E_0 is determined from the energy at the half-height of the U L_{III} absorption edge. $I_0(k)$ was determined by fitting a 7 knot spline through data up to 14 $Å^{-1}$.[11]

Because of a monochromator glitch in the UF_4 data at about 17 475 eV, our comparative study will use only the limited k-range up to about 9 $Å^{-1}$. However, if the complete range of the UO_2 data, up to 14 $Å^{-1}$ is used in the Fourier transform (FT), then the real space EXAFS result for UO_2 is almost identical in terms of peak position and peak size to those reported earlier in Ref. 5 (Fig. 2) and Ref. 6 (Fig. 3).

Both samples were single crystals. The uranium dioxide sample was part of the depleted UO_2 single crystals obtained by Los Alamos Scientific Laboratory (LASL, now Los Alamos National Laboratory, LANL) from Pacific Northwest Laboratory in 1969.

They are the same samples used and characterized in recent thermal conductivity measurements. An optical photograph, Laue diffraction pattern and additional details regarding sample chemistry are referenced therein.[16] The uranium tetrafluoride sample was originally prepared at

[a)]On sabbatical at the Glenn T. Seaborg Center, LBNL, during FY2014. Author to whom correspondence should be addressed; electronic mail: tobin1@llnl.gov

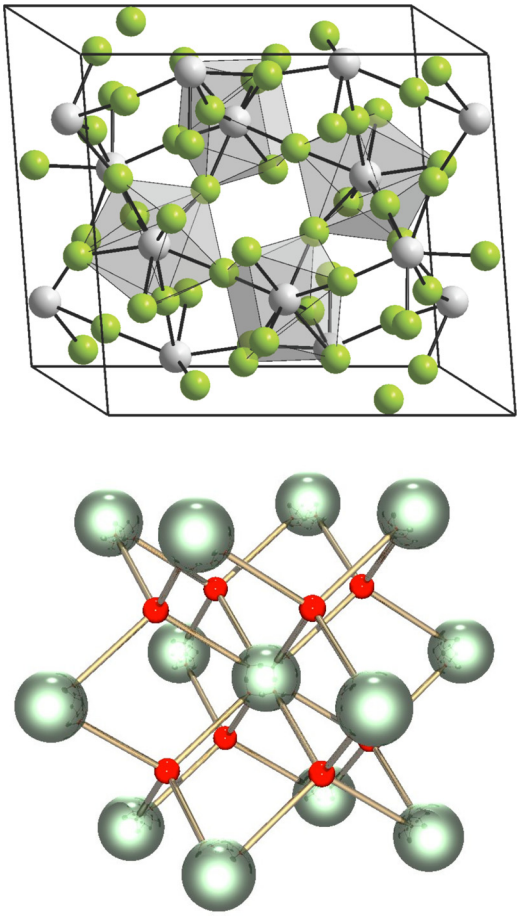

FIG. 1. (Color online) Top: UF_4 is monoclinic, with two types of U. The image is from Wikipedia, specifically File:Kristallstruktur Uran(IV)-fluorid.png. Bottom: UO_2 is a fluorite (cubic) structure. The image is from Wikipedia, i.e., Cadmium at en.wikipedia.

Y12/Oak Ridge National Laboratory, similarly to our previous uranium sample.[17]

In the region of the absorption edge, it is possible to observe the large spectral features known as XANES (Fig. 2). For the U L_{III} ($2p_{3/2}$) edge, the threshold is near 17 160 eV. The experimental spectra in Fig. 2 for UO_2 and UF_4 duplicate the earlier results of Kalkowski *et al.* for both compounds.[18] In general, XANES gives a measure of the unoccupied density of states.[19] This is exemplified in Fig. 2, by comparing the experimental XANES spectra with simulated spectra, using the 6 d state distributions calculated in Ryzhkov's cluster models.[20,21] Here, Doniach-Sunjic lineshapes[22] have been used, with the asymmetry parameter (α) of 0.3 and lifetime width (Γ) of 4 eV, with $\Gamma = 1/2$ the full width half maximum of the Lorentzian component. The underlying assumption is that each state generates a contribution of equal intensity. As can be seen, there is a good agreement between the experimental and simulated spectra. The UO_2 and UF_4 experimental XANES spectra shown in Fig. 2 are similar, with some tantalizing suggestions of differences; for instance, the first inflection point of the UF_4 spectrum is 1.4 eV higher (at 17 167.4 eV) than that of the UO_2 spectrum (defined to be 17 166.0 eV), and the peak in the absorption is 0.3 eV higher in UF_4 (17 172.5 eV)

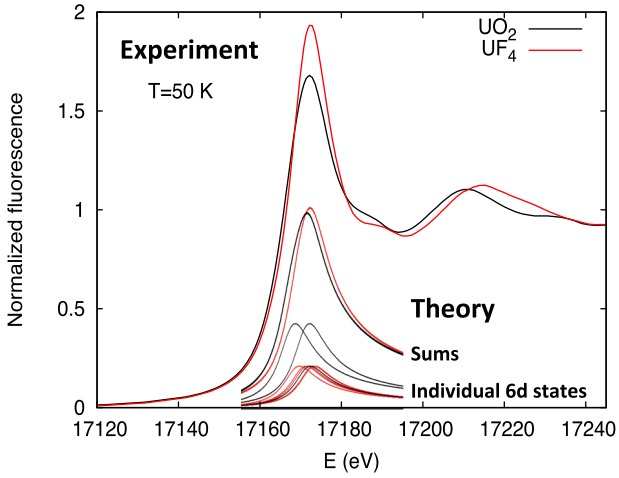

FIG. 2. (Color online) L_3 XANES of uranium dioxide and uranium tetrafluoride, plus simulated spectra based upon the cluster models of Ryzhkov *et al.* (Refs. 20 and 21). E (eV) is the experimental excitation photon energy, from the beamline monochromator. The experimental energy scale is directly from the measurements, with no shifting. The theory energy scales are directly from the energy scales for the unoccupied density of states in Refs. 20 and 21, again with no shifting. The experimental pair and theory pair have been arbitrarily aligned relative to each other, but with matching energy ranges. The theory insert is 40 eV wide. The intensity zeros are the same for the experiment and theory. The theory intensity is arbitrarily scaled relative to the experiment.

compared to UO_2 (17 172.2 eV). Note that the values for UO_2 are consistent with those reported in Ref. 5, given the difference in energy calibration. The differences reported here between the UF_4 and the UO_2 spectra may indicate increased localization (or decreased covalency) in UF_4 relative to UO_2, but differences in the lineshape may indicate another alternative, such as increased crystal field splitting in UO_2 relative to UF_4. The resolution in these measurements is, however, insufficient to achieve a convincing differentiation. (The effective resolution in these measurements is limited by the lifetime broadening of the $2p_{3/2}$ core hole of about 10 eV.) However, measurements made in the resonant x-ray emission spectroscopy (RXES, Refs. 23 and 24) mode do exhibit clear differences, but that will be discussed elsewhere.[25] As the energy of the incoming photons rises

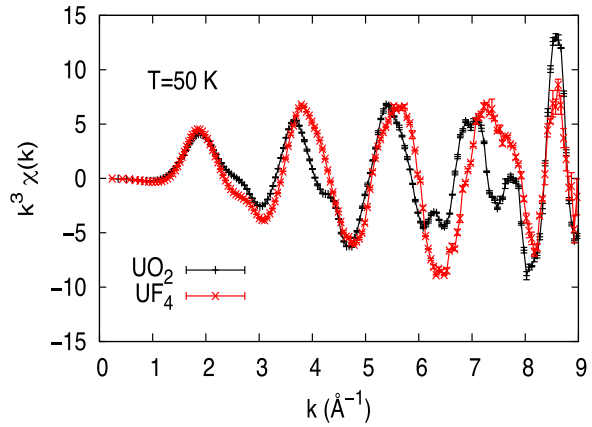

FIG. 3. (Color online) Plot of the EXAFS oscillations vs the wave vector of the outgoing electron. Error bars were determined by averaging three scans.

substantially above the edge, the spectral features diminish in size and change in nature, becoming the oscillations associated with EXAFS.

EXAFS is a powerful analytical technique for the determination of interatomic distances and structure, with results ranging from water[26] through Pu (Ref. 27) and beyond.[28,29] EXAFS oscillations dominate the absorption spectrum about 20 eV above the absorption edge and are caused primarily by the scattering of emitted electrons from nearby atoms. While initially measured as a function of the incoming photon energy, this curve is subsequently converted into a normalized plot of the EXAFS function χ (Refs. 10 and 11) versus the wave-vector of the outgoing electrons (Fig. 3). It is useful to begin the data analysis in the most simple and direct fashion, by applying a Fourier transform to the oscillations in k-space, which then produces a spectrum in r-space. This spectrum is similar to a partial radial pair distribution function (RDF). It is, however, different from an RDF in some important respects. Most importantly, since EXAFS is an interference effect, both the amplitude and the phase of the photoelectron are important, and are varied both by the absorption atom and by the backscattering atoms. Because of these complications, peaks in r-space are shifted from the values of the actual pair distances, and interference effects can also cause peaks and dips in unexpected places in the spectrum. Moreover, the backscattering amplitudes are a function of k (and therefore r), causing more differences with an actual RDF. Fortunately, the complex backscattering functions are well reproduced by codes such as FEFF,[13] and actual metrical data can be gleaned from careful fits to these spectra as described below. In spite of these issues, it remains instructive to consider the raw spectra in the absence of any fitting with these complications in mind.

Consider the transforms in Fig. 4. Our EXAFS transform for UO_2 agrees qualitatively with those for UO_2 reported earlier: specifically Fig. 2 in Ref. 5 and Fig. 3 of Ref. 6. The major difference is the reduction of the peak near 4 Å, relative to that reported in Refs. 5 and 6. We attribute this reduction to the limited width of our data set, i.e., only up to about 9 $Å^{-1}$, as shown in Fig. 3. (See the Experimental discussion.) This leads us to preliminarily assign the two largest features to the nearest neighbor oxygen atoms (R = 2.36 Å) and the next nearest neighbor uranium atoms (R = 3.85 Å), following Refs. 5 and 6. Thus, in the UO_2, with its highly ordered (fluorite) structure and single site for U, it is possible to easily see both nearest neighbor (O) and second nearest neighbor (U) peaks. However, the UF_4 behavior is different: here, only a single strong transform peak is observed in Fig. 4, near r = 2 Å. There are weak maxima at larger r values, but clearly nothing as strong as the peak in the UO_2 transform near r = 4 Å. Thus, it appears that only the nearest neighbor backscattering peak is clearly observed. This result suggests that for UF_4, in a monoclinic structure with two U sites, only the nearest neighbor F ring produces a clear peak, while the U-U scattering washes out due to the two sites and multiple U-U distances. However, this hypothesis needs to be tested with a more sophisticated and accurate analysis, as described below.

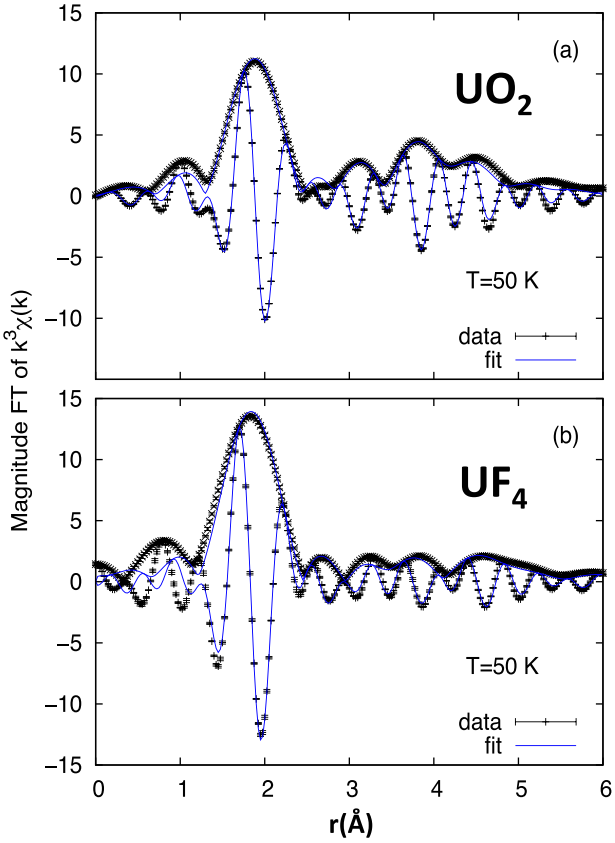

FIG. 4. (Color online) FT of $k^3\chi(k)$ vs r data and the results of the data fits for (a) UO_2 and (b) UF_4. The experimental data between 2.5 and 9.0 $Å^{-1}$, shown in Fig. 3, were transformed using a 0.3 $Å^{-1}$ wide Gaussian window. Both the FT amplitude (+) and amplitude squared (X) are shown. Errors were determined by averaging the transforms from each of the three scans. These spectra have not been phase shift corrected. The fit results are shown as smoothly curving lines.

As mentioned above, a monochromator glitch at about 17475 eV limited the useful k-range of UF_4 data to about 9 $Å^{-1}$. Since the EXAFS from UO_2 has been measured many times in the past, we limited the k-range of both samples to 9 $Å^{-1}$ to make a direct comparison to the UF_4 results. Figure 4 shows the corresponding FT results, together with fits, which are described below.

Fits to the data were performed in r-space, with errors determined using a Monte Carlo method.[30] The fitting models were based on the nominal crystal structure of each compound, and as such, the model for UO_2 (fcc cubic)[31] is much simpler that for UF_4 (monoclinic).[7] In each case, the scattering amplitude of each shell was constrained to that of the nominal crystal structure, using a single amplitude reduction factor, S_0^2, for all the shells in each EXAFS spectrum. With such a model, any deviations between the actual local structure and the fitting model would be reflected only in the measured pair distances and by enhancements in the pair-distribution variances, σ^2, and to a lesser degree in the fitted S_0^2. Since UO_2 forms in a high symmetry, the first few scattering shells are distinct, with 8 U-O neighbors nominally at 2.368 Å, 12 U-U neighbors at 3.867 Å, and 24 U-O neighbors at 4.534 Å (see Table I). Fits to the EXAFS data utilized a fitting model based on these scattering shells, as well as

TABLE I. Results from fits to the UO_2 and UF_4 data. Fit range is between 1.5 and 5.0 Å for the UO_2 data and between 1.5 and 6.0 Å for the UF_4 data. The k_3-weighted data sets are both transformed between 2.5 and 9.0 $Å^{-1}$ and Gaussian narrowed by 0.3 $Å^{-1}$. Fit models are based on the nominal crystal structures (Refs. 7 and 31) using single scattering shells as reported here and also including multiple scattering. The XRD results summarize here give the pair distance and the distribution variance of each shell from the fitting model. For instance, in UF_4, each of the two uranium sites have 8 F neighbors ranging in distance from 2.23 to 2.35 Å, with a distribution variance as shown, compared to the nearest neighbor U-O shell in UO_2, which has all eight at about 2.368 Å. Note that the EXAFS variances include both thermal and static components. For the analysis of UO_2, ten parameters were varied of the 16.5 independent data points [using Stern's rule (Ref. 32)], corresponding to 6.5 degrees of freedom, resulting in a statistical χ^2 of 1.87, and R(%) (as defined in Ref. 11) of 9.95%. For the analysis of UF_4, these values were as follows: ten variables, 20.6 independent data points, 10.6 degrees of freedom, $\chi 2 = 2.43$, and R(%) = 9.95%.

	N	σ^2_{XRD} (Å^2)	R_{XRD} (Å)	σ^2 (Å^2)	R (Å)
			UO_2		
U-O	8	—	2.368	0.002(1)	2.361(9)
U-U	12	—	3.867	0.000(1)	3.87(1)
U-O	24	—	4.534	0.003(3)	4.50(2)
ΔE_0		−15.9(9)			
S_0^2		0.82(9)			
			UF_4		
U-F	8	0.0012	2.273	0.003(1)	2.282(6)
U-F	9	0.0106	4.204	0.012(8)	4.24(3)
U-U	8	0.0015	4.505	0.004(2)	4.48(8)
ΔE_0		−17.2(7)			
S_0^2		0.90(8)			

including multiple scattering paths within the fit range. Fit results are shown in Table I and Fig. 4. The fits to the UF_4 data are also relatively straightforward, but since these data can't resolve pairs closer than $\Delta r \approx \pi/2k_{max} \approx 0.2$ Å together, a significant enhancement to the σ^2 values occurs due to static displacements of each scattering shell relative to a well ordered system like UO_2. A fitting model was chosen using three single-scattering shells with U-F, another U-F, and U-U pairs. Grouping the expected distances into the first 8, 9, and 8 neighbors, respectively, average pair distances and distribution variances were determined from the x-ray diffraction (XRD) data for comparison to the EXAFS results, as shown in Table I, with the corresponding fit shown in Fig. 4.

As shown in Fig. 4, there are distinct differences in the EXAFS data for UO_2 and UF_4. Interestingly, even though the static nearest-neighbor U-O distribution is much sharper in UO_2 than the U-F distribution in UF_4, the larger scattering factor of fluorine still generates a larger first peak in the r-space spectrum of UF_4 than in UO_2. On the other hand, the relatively broad static distributions of the second U-F-shell and the U-U-shell generate smaller features in the EXAFS beyond 3 Å. These differences are consistent with the nominal crystal structures as reflected by the fit results. In particular, the scattering shell distances from the EXAFS fits are very consistent with the models generated from the nominal crystal structures. Moreover, although data were only obtained at a single temperature of 50 K and we therefore do not know the exact thermal contribution to the EXAFS distribution widths, the results from the fits are qualitatively consistent with the expected static displacements from the fitting model in that those from UO_2 are small and consistent with scattering widths limited by thermal vibrations and those from UF_4 are enhanced by amounts consistent with the expected static distributions in the fitting model. Additionally, the measured S_0^2 values are both near 0.9, consistent with most other previous EXAFS results.

The local structure of UF_4 is consistent with the long-range structure derived from diffraction data, confirming the quality of the UF_4 sample and the structural differences between UF_4 and UO_2. While the XANES measurements suggest that there are differences between the UF_4 and UO_2 6d unoccupied density of states, the resolution of these differences and fuller discussion of the underlying causes will need to wait for the higher resolution of the RXES measurements.[25]

ACKNOWLEDGMENTS

Lawrence Livermore National Laboratory is operated by Lawrence Livermore National Security, LLC, for the U.S. Department of Energy, National Nuclear Security Administration under Contract No. DE-AC52-07NA27344. Work at Lawrence Berkeley National Laboratory (C.H.B. and D.K.S.) was supported by the Director, Office of Science, Office of Basic Energy Sciences (OBES), Division of Chemical Sciences, Geosciences, and Biosciences of the U.S. Department of Energy under Contract No. DE-AC02-05CH11231. The XANES and EXAFS data were collected at BL-11-2 at SSRL. The Stanford Synchrotron Radiation Lightsource is a national user facility operated by Stanford University on behalf of the DOE, Office of Basic Energy Sciences. The UF_4 sample was originally prepared at Oak Ridge National Laboratory and provided to LLNL by J. S. Morrell of Y12.[4] The images in Fig. 1 are from Wikipedia, specifically File:Kristallstruktur Uran(IV)-fluorid.png and Cadmium at en.wikipedia. JGT wishes to thank (1) Glenn Fox and the PRT Program at LLNL for support during his sabbatical at LBNL; (2) D.K.S. for his hosting of the sabbatical at GTSC/LBNL; and (3) C.H.B. for the opportunity to learn new hard x-ray skills and collect data in the middle of the night again. The authors thank Eric D. Bauer and Mark T. Paffett of LANL for making the UO_2 sample available to us.

[1]I. D. Prodan, G. E. Scuseria, and R. L. Martin, Phys. Rev. B **76**, 033101 (2007).
[2]S.-W. Yu, J. G. Tobin, J. C. Crowhurst, S. Sharma, J. K. Dewhurst, P. Olalde-Velasco, W. L. Yang, and W. J. Siekhaus, Phys. Rev. B **83**, 165102 (2011).
[3]J. G. Tobin and S.-W. Yu, Phys. Rev. Lett. **107**, 167406 (2011).
[4]S.-W. Yu and J. G. Tobin, J. Electron Spectrosc. Relat. Phenom. **187**, 15 (2013).
[5]S. D. Conradson, D. Manara, F. Wastin, D. L. Clark, G. H. Lander, L. A. Morales, J. Rebizant, and V. V. Rondinella, Inorg. Chem. **43**, 6922 (2004).
[6]S. D. Conradson *et al.*, Phys. Rev. B **88**, 115135 (2013).
[7]A. C. Larson, R. B. Roof, Jr., and D. T. Cromer, Acta Crystallogr. **17**, 555 (1964).
[8]"Experimental station 11-2," http://www-ssrl.slac.stanford.edu/beamlines/bl11-2/.

[9]J. J. Bucher, P. G. Allen, N. M. Edelstein, D. K. Shuh, N. W. Madden, C. Cork, P. Luke, D. Pehl, and D. Malone, Rev. Sci. Instrum. **67**, 3361 (1996).
[10]T. M. Hayes and J. B. Boyce, *Extended X-Ray Absorption Fine-Structure Spectroscopy* (Academic, New York, 1982), Vol. 37, p. 173.
[11]G. G. Li, F. Bridges, and C. H. Booth, Phys. Rev. B **52**, 6332 (1995).
[12]"RSXAP analysis package," http://lise.lbl.gov/RSXAP/
[13]A. L. Ankudinov and J. J. Rehr, Phys. Rev. B **56**, R1712 (1997).
[14]D. Haskel, "FLUO: Correcting XANES for self absorption in fluorescence measurements," http://www.aps.anl.gov/xfd/people/haskel/fluo.html, 1999.
[15]C. H. Booth and F. Bridges, Phys. Scr. **T115**, 202 (2005).
[16]K. Gofryk *et al.*, Nat. Commun. **5**, 4551 (2014).
[17]S. W. Yu and J. G. Tobin, J. Vac. Sci. Technol. A **29**, 021008 (2011).
[18]G. Kalkowski, G. Kaindl, W. D. Brewer, and W. Krone, Phys. Rev. B **35**, 2667 (1987).
[19]B. K. Teo, *EXAFS Basic Principles and Data Analysis* (Springer Verlag, New York, 1986).
[20]Yu. A. Teterin, K. I. Maslakov, M. V. Ryzhkov, O. P. Traparic, L. Vukcevic, A. Yu. Teterin, and A. D. Panov, Radiochemistry **47**, 215 (2005).
[21]A. Yu. Teterin, Yu. A. Teterin, K. I. Maslakov, A. D. Panov, M. V. Ryzhkov, and L. Vukcevic, Phys. Rev. B **74**, 045101 (2006).
[22]J. G. Tobin and F. O. Schumann, Surf. Sci. **478**, 211 (2001).
[23]C. H. Booth *et al.*, Proc. Natl. Acad. Sci. **109**, 10205 (2012).
[24]C. H. Booth *et al.*, J. Electron Spectrosc. Relat. Phenom. **194**, 57 (2014).
[25]J. G. Tobin, C. H. Booth, D. Sokaras, and T. C. Weng, "Oxidation and crystal field effects in uranium" (unpublished).
[26]K. R. Wilson, J. G. Tobin, A. Ankudinov, J. Rehr, and R. J. Saykally, Phys. Rev. Lett. **85**, 4289 (2000).
[27]P. G. Allen, A. L. Henderson, E. R. Sylwester, P. E. A. Turchi, T. H. Shen, G. F. Gallegos, and C. H. Booth, Phys. Rev. B **65**, 214107 (2002).
[28]E. Galbis, J. Hernandez-Cobos, C. den Auwer, C. Le Naour, D. Guillaumont, E. Simoni, R. R. Pappalardo, and E. Sanchez Marcos, Angew. Chem., Int. Ed. **49**, 3811 (2010); Angew. Chem. **122**, 3899 (2010).
[29]K. E. Knope and L. Soderholm, Chem. Rev. **113**, 944 (2013).
[30]C. H. Booth and Y.-J. Hu, J. Phys.: Conf. Ser. **190**, 012028 (2009).
[31]R. W. G. Wyckoff, *Crystal Structures*, 2nd ed. (Interscience, New York, 1964).
[32]E. A. Sterne, Phys. Rev. B **48**, 9825 (1993).